Shock-Induced C-N-S Tridoped TiO_2 with Improved Photocatalytic Activity Under Visible Light

Chunxiao Xu[1], Jianjun Liu[2], Naifu Cui[1] and Pengwan Chen[1,*]

[1]*School of Materials Science and Engineering, Beijing Institute of Technology, Beijing 100081, China*

[2]*State Key Laboratory of Chemical Resource Engineering, Beijing University of Chemical Technology, Beijing 100029, China*

Abstract: Using metatitanic acid (H_2TiO_3) and thiourea (CN_2H_4S) as titanium precursor and dopant source respectively, a visible-light responsible non-metal C-N-S tridoped TiO_2 photocatalyst is prepared by shock loading. X-ray powder diffraction (XRD), transmission electron microscopy (TEM), X-ray photoelectron spectroscopy (XPS) and UV-visible diffuse reflectance spectroscopy (UV-Vis DRS) are employed to characterize the crystalline structure, morphology, chemical composition and optical property of recovered samples. The results indicate the metatitanic acid transforms to pure anatase phase by shock wave and that the average size of particles is 3-5 nm. The as-synthesized TiO_2 nano-particles are well dispersed and possess large surface area (309.02 m^2/g), and the edge adsorption wavelength of the samples exhibits slight red shifts with corresponding energy gap reduced to 3.16 eV. Carbon forms carbonate on the surface of TiO_2, N may coexist in the forms of substituted N (N-O-Ti) and interstitial N (O-Ti-N) in TiO_2, and S^{6+} is incorporated into the lattice of TiO_2 through substituting titanium atoms. The photocatalytic activities of the as-synthesized samples are evaluated for the degradation of Rhodamine B under simulated sunlight irradiation. Results reveal that these C-N-S tridoped TiO_2 exhibit higher photocatalytic degradation activities than that of undoped TiO_2 samples and achieve an 83% removal rate for RB dye under the visible light irradiation for 70 min with the thiourea-to-metatitanic acid mass of 2:1 and flyer velocity 2.52 $km \cdot s^{-1}$, which is mainly attributed to the synergistic effects of well-formed anatase phase, high specific surface area and band gap narrowing resulting from C-N-S tridoping.

Keywords: Shock wave, titanium dioxide, non-metal doped, photocatalysis.

1. INTRODUCTION

It is well known that titania is widely applied in the solar energy conversion, air purification, and waste water treatment as a most effective photo-functional material [1,2]. But since the band gap of TiO_2 is large (Eg=3.2eV), it is only active in ultraviolet region accounting for 3-5% of the overall solar energy. Therefore, it is much more important to enhance the visible light activity of TiO_2 photocatalyst. For this reason, many modifications have been made on TiO_2 matrix such as surface photosensitization, doping of TiO_2 with some ions and coupling with other narrow semiconductor [3-5]. Recently, TiO_2 doping with nonmetal elements has been considered as an effective approach to extend the light absorption of TiO_2 to visible region [6]. From then on, many attempts have been done on non-metal doped TiO_2, such as B [7], C [8], N [9], F [10] and S [11], which indicating that this TiO_2-based catalyst exhibits relatively high visible light photocatalytic activity due to the band gap narrowing. More recently, owing to the synergistic effect of doping element, the visible light response and photocatalytic activity could be further improved for a photocatalyst with simultaneous multi-dopants. Rengifo-Herrera *et al*. [12] fabricated N-S codoped P25 by manual grinding of thiourea or urea with pure P25 for *E. coli* inactivation. Zhou and Yu [13] reported that the C-N-S tridoped TiO_2, prepared *via* mixing xerogel and thiourea, exhibited about more than six times removal efficiency of formaldehyde than those of undoped TiO_2 and Degussa P25 under daylight illumination.

Shock wave action of high temperature, high pressure and high strain rate lasting for very short time (~10^{-6} s) will cause a series of catastrophic changes of chemical and physical properties of materials [14]. Under shock wave action, the organic dopant can be decomposed and diffused into the lattice of TiO_2, so the shock doping combined with shock-induced chemical reaction and phase transition may be a new method to extend the absorption edge into visible light and enhance the photocatalytic activity of TiO_2. Compared with other TiO_2 doping method, such as sputtering method, solvothermal method, metal organic chemical vapor deposition method [15-17], etc. This method does not need high ambient temperature, long reaction time and complicated reaction process, and can achieve high doping concentration. Until now, there are few reports concerning TiO_2 doping induced by shock wave. Chen *et al*. [18-20] prepared nitrogen-doped

*Address correspondence to this author at the School of Materials Science and Engineering, Beijing Institute of Technology, Beijing 100081, China; Tel: 86-13910118789; Fax: 86-10-68912470; E-mail: pwchen@bit.edu.cn

E-ISSN: 2410-4701/15

titania by shock loading, the maximum concentration of nitrogen of doped TiO_2 is 13.45 at. % much higher than that of current reports, suggested that shock doping could be a novel and efficient preparation route for TiO_2 semiconductor.

In this study, a steel flyer is driven by the detonation of nitromethane (CH_3NO_2), in order to produce high temperature and high pressure to complete shock-induced C-N-S tridoped TiO_2. Under shock action, the organic dopant thiourea can be decomposed and diffused into the lattice of TiO_2. The structures and photocatalytic activities of the doped TiO_2 are characterized and evaluated, respectively.

2. EXPERIMENTAL

2.1. Synthesis of C-N-S Tridoped TiO_2

Metatitanic acid (HT, H_2TiO_3) is chosen as titanium precursor while thiourea (TU, CN_2H_4S) is used as doping carbon, nitrogen and sulfur resource. All chemicals are purchased from Beijing Chemical Reagents Company without any further purification. The sample is a mixture with the TU-to-HT mass ratios of 0.25:1 and 2:1, respectively. The scheme of shock-loading apparatus is shown in Figure **1**. The steel flyer is propelled to a high velocity ranging from 1 to 3 $km \cdot s^{-1}$ depending on the charge mass by detonation of the main charge of nitromethane (CH_3NO_2), initiated by booster charge of 8701 explosive. The steel flyer impact the container with the samples subjecting to shock wave compression. The approximate calculation on the shock pressure and temperature can be described elsewhere in detail [21]. In this study, flyer velocity of 3.07 and 2.52 $km \cdot s^{-1}$ are selected as the loading condition and the experimental conditions are shown in Table **1**.

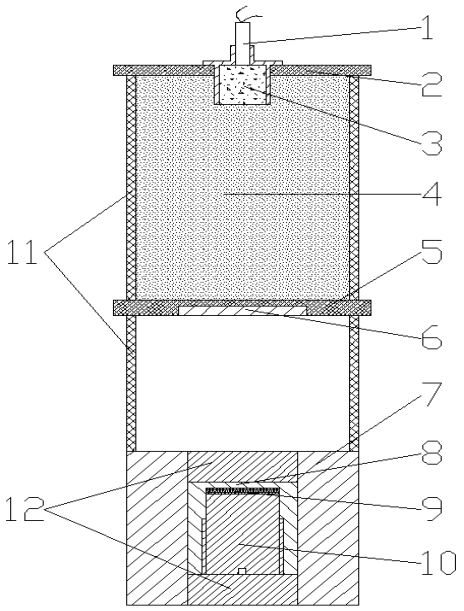

Figure 1: Scheme of shock-loading apparatus.

(1) detonator; (2) upper cover; (3) booster charge; (4) nitromethane; (5) bottom cover; (6) flyer; (7) steel protection tube; (8) copper sample container; (9) sample; (10) copper screw lid; (11) PVC plastic tube; (12) steel momentum block.

2.2. Characterization of Photocatalyst

The phase compositions of the recovered samples are determined on an X-ray powder diffraction (XRD) (Bruker D8 Advance) using Cu Kα radiation (λ= 0.15406 nm) at 40 kV work voltage and 200 mA work current in a 2θ range of 10-90°. The crystallite size is estimated from the XRD patterns by using the Scherrer formula D=0.89λ/(βcosθ), where D is the crystal size in nanometers, λ is the Cu Kα wavelength (0.15406 nm), β is the half-width of the peak in radians, and θ is the corresponding diffraction angle. The particle morphology is observed with a JEM-2010 transmission electron microscopy (TEM) at an accelerating voltage of 200 kV. BET specific surface area is obtained using Quadrasorb SI-MP measurements at 77 K. Before measurement, all the samples are degassed under vacuum at 300 ^{o}C for 5 h. The surface chemical

Table 1: Preparation Conditions of C-N-S Tridoped TiO_2 Photocatalyst

Sample	Flyer Velocity (km/s)	Mass Ratios of TU/HT	Initial Density ρ_0 (g/cm^3)	ρ_0/ρ_{00} (%)	Shock Pressure (GPa)	Shock Temperature (K)
622	3.07	0.25	1.74	60.50	26.88	758.01
619	3.07	2.00	1.46	81.70	24.44	613.28
606	2.52	0.25	1.78	61.80	20.32	657.77
603	2.52	2.00	1.52	85.10	18.96	517.88

compositions and bonding states of the photocatalysts are probed by X-ray photoelectron spectroscopy (XPS) analysis on a Thermo ESCALAB 250 spectrometer. The UV-vis diffuse reflectance spectra (DRS) is obtained using a Shimadzu UV-Vis 250 IPC spectrophotometer equipped with an integrating sphere assembly with $BaSO_4$ as the reflectance standard.

2.3. Evaluation of Photocatalytic Activity

The activities of the as-synthesized samples are evaluated by the photocatalytic degradation of Rhodamine B (RB) under simulated sunlight irradiation. All the photocatalytic experiments are performed in black box at ambient temperature and pressure. A 500 W Xe lamp is used as the light source and the visible wavelength is controlled through a 420 nm cut filter (LF420, China), which kept at about 15 cm above the liquid level. Typically, the aqueous RB-catalyst suspension is prepared as follows. A 40 mg sample of the catalyst is dispersed in 20 mL of deionized water by ultrasonication for 15 min. And then 20 mL of aqueous solution containing RB dye with an initial concentration of 20 $mg \cdot L^{-1}$ is added into the above suspension. Prior to irradiation, the mixture is stirred for 60 min in the dark and allow the adsorption-desorption equilibrium between dye and photocatalyst surface. Under stirring, aliquots of a small amount of suspension (about 4 mL) is taken out at every 10 min under visible light irradiation, After the irradiation and removal of the catalyst particles by centrifugation, the residual amount of RB in the solution is analyzed using a 721 spectrophotometer (made in China) to measure the change of RB concentration with irradiation time based on Lambert-Beer's law. The percentage of degradation is indicated as A/A_0, Here, A is the absorbance of RB solution at each irradiation time interval of the main peak of the adsorption spectrum, and A_0 is the absorbance of the initial concentration when the adsorption-desorption equilibrium was achieved. For comparison, the photocatalytic activity of raw material H_2TiO_3 and the undoped TiO_2 nanoparticles is also conducted under the identical experimental conditions.

3. RESULTS AND DISCUSSION

3.1. XRD, TEM and BET Analysis

The XRD patterns of shock-recovered samples are shown in Figure **2**. Obvious diffraction peaks attributed to the anatase phase (JCPDF 21-1272) appear while there is no other phase for all the C-N-S tridoped TiO_2. It indicate that metatitanic acid can transform to pure anatase phase together with the decomposition of dopant thiourea under shock action. The decomposed product of dopant source thiourea containing C, N or S species may incorporate into TiO_2 lattice with enforced diffusion effect caused by shock wave. The average crystal size is estimated from the broadening of the corresponding X-ray diffraction peaks by Scherrer formula. The physicochemical properties of the as-synthesized samples are listed in Table **2**. As seen from Table **2**, the average crystallite size of the C-N-S tridoped TiO_2 is about 4.5 nm and the particle size has

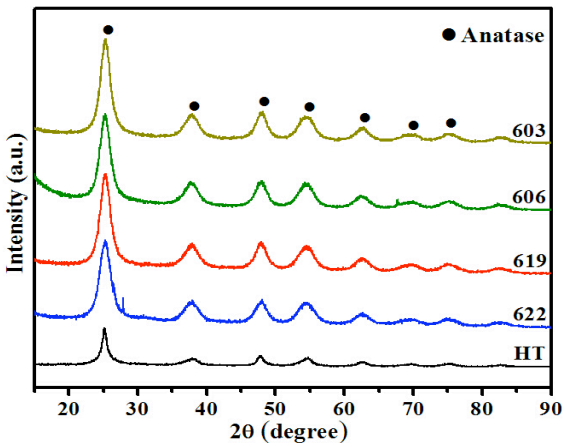

Figure 2: XRD patterns of C-N-S tridoped TiO_2 catalysts with different flyer velocities.

Table 2: Results of C-N-S Tridoped TiO_2 Photocatalysts

Sample	Flyer velocity (km/s)	Mass ratios of TU/HT	XPS result			S_{BET} (m^2/g)	Grain size[a] (nm)	E_g[b] (eV)	$(A_0-A)/A_0$[c] (%)
			C1s (at%)	N1s (at %)	S2p (at %)				
622	3.07	0.25	42.55	3.97	1.16	285.20	4.48	3.16	29.70
619	3.07	2.00	27.76	2.37	1.06	309.02	4.64	3.24	32.20
606	2.52	0.25	29.53	2.04	1.23	253.36	4.61	3.27	38.60
603	2.52	2.00	28.70	2.21	0.86	266.27	4.58	3.20	83.00

[a] Derived from XRD patterns.

[b] Band gap energy, calculated using the transformed Kubelka–Munk function.

[c] Represent the photocatalytic degradation rate. A is the absorbance values of RB.

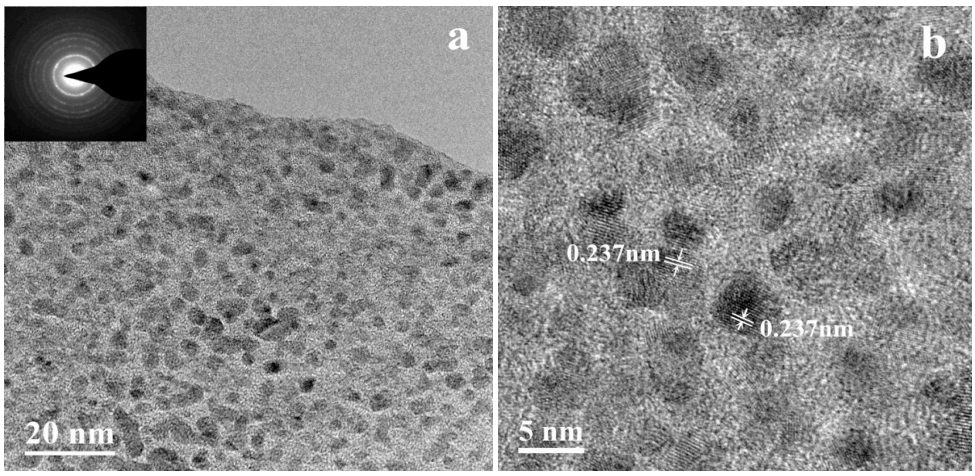

Figure 3: HRTEM images of the sample 619.

negligible variation when improving the speed of flyer. Thus, it can be concluded that samples possess a good crystallinity with the flyer velocity of 2.52 $km \cdot s^{-1}$ and the improvement of impact energy with the flyer velocity of 3.07 $km \cdot s^{-1}$ has a less influence on the crystallization and growth of TiO_2 nanosized-particles.

Figure **3a** shows that the average crystalline size of sample 619 is about 3-5 nm, which is in agreement with the calculation results from XRD patterns in Figure **2**. It is noted from the selected area electron diffraction (SAED) patterns of TiO_2 that the sample of 619 is pure anatase which can be further validated by the HRTEM image in Figure **3b**. It shows clear lattice fringes, which allows for identification of crystal-lographic spacing. The fringe spacing of 0.237 nm matches that of the (004) crystallographic plane of TiO_2 anatase. Additionally, the as-synthesized TiO_2 spherical particles are well dispersed. This is mainly due to the dehydration expansion of metatitanic acid under shock wave action during very short time, which can cause uniform TiO_2 particles have no time to grow up and inhibit the aggregation of particles. The specific surface area of the samples shown in Table **2** is about 260 m^2/g, which may possess large contact area of active site and reactant, and thus could enhance photocatalytic degradation activity of organic dyes.

3.2. XPS Analysis

Figure **4** illustrates the high-resolution XPS spectra of C 1s, N 1s and S 2p of the C-N-S tridoped TiO_2 photocatalysts treated by shock wave at different conditions. Using XPSPEAK soft, different kinds of chemical states in one region are deconvoluted into corresponding peaks. The XPS results are summarized in Table **2**. Figure **4a** shows that all the samples have a peak located at 284.7 eV which is assigned to the adventitious carbon or carbon residues from the organic precursor [22]. In addition, weak peaks positioned at 286.2 and 288.5 eV are present in all the samples. Wang *et al*. [23] indicated that these peaks around 286 and 288 eV were assigned to C-O, O=C-O and C-N bonds, suggesting the formation of carbonate species which could act as photosensitizer to enhance the visible-light absorption. While Cheng *et al*. [24] considered that the weak peak located at 288.2 eV could be ascribed to O=C bond of carbonate species, which could induce the narrowing of the band gap and could response to visible light.

Figure **4b** shows the XPS spectra for the N 1s region of C-N-S tridoped TiO_2 sample and its fitting curves. The peaks around 400eV are assigned to the molecularly chemisorbed γ-N(N-H, N-N, N-O bonds), such as NH_3、N_2 and NO_x [25, 26]. Wang [27] indicated that the peaks at 401.8 or 401.4eV were attributed to the interstitial N-doping in the Ti-O-N sites. While Wei [28] considered that the peak at 401.5eV was attributed to the O-Ti-N sites substitutionally incorporated into the TiO_2 lattice. The peaks around 407.1 eV belongs to NO_2^- or NO_3^- species [29-31], and probably caused by the further oxidation of NO_x during shock wave impact.

Figure **4c** shows the high resolution XPS spectra of the S 2p region taken for the C-N-S tridoped TiO_2 sample. Rengifo *et al*. [32] indicated that the peaks at 168.7 and 169.9eV were attributed to binding energy of S^{6+}, bonding on the surface of TiO_2 with the species of SO_4^{2-}. Ju *et al*. [33] explained that the peak at 168.4eV could be deconvoluted into S^{6+} $2p_{3/2}$ and S^{6+} $2p_{1/2}$ positioning at 168eV and 169.3eV, respectively. In this study, the as-synthesized TiO_2 has been washed with distilled water several times, so the peak at 168.5 eV

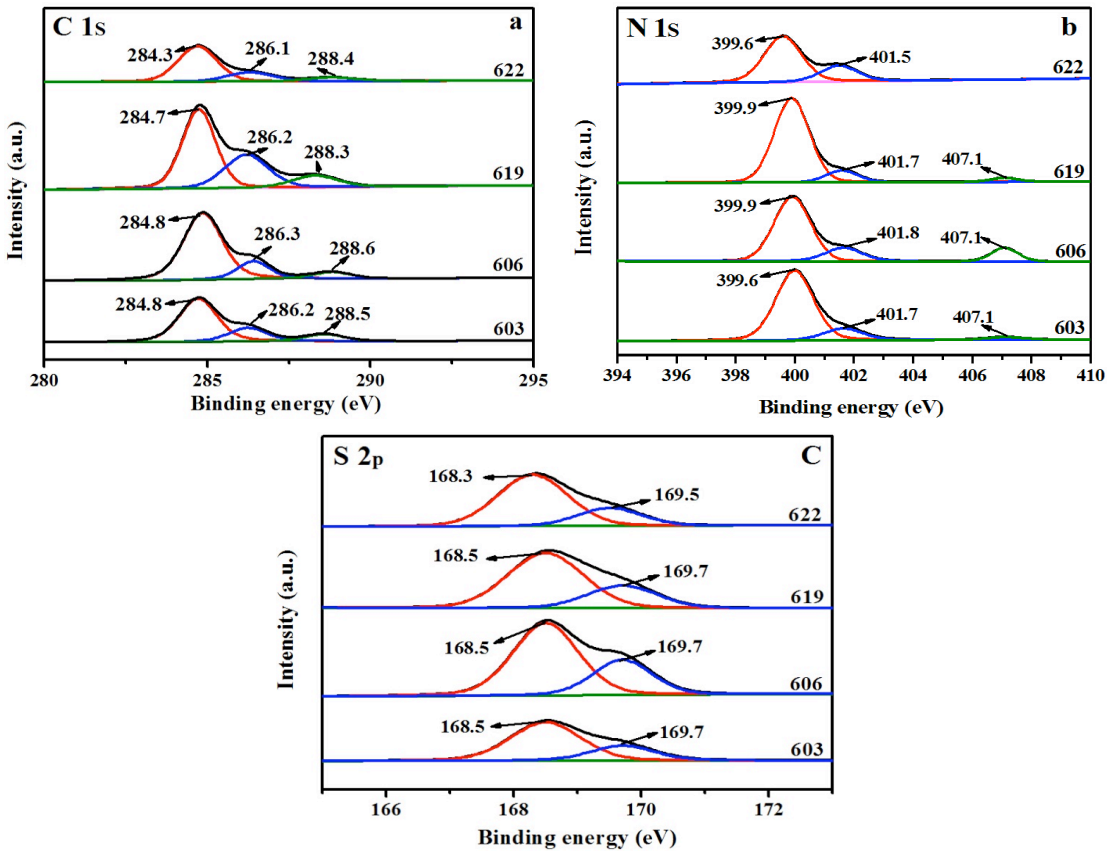

Figure 4: XPS high-resolution spectra of C 1s (**a**), N 1s (**b**) and S 2p (**c**) of the C-N-S tridoped TiO_2 photocatalysts with different flyer velocities.

and 169.7 eV can be attributed to the cationic sulfur doping, namely, S^{6+} substitutes for the lattice Ti^{4+}. Ohno *et al*. [34] demonstrated that cationic S-doped TiO_2 absorbed visible light more strongly than N and C doped TiO_2, leading to high photocatalytic activity under visible light.

3.3. UV-vis DRS Analysis

The optical property of the as-synthesized C-N-S tridoped TiO_2 photocatalysts, together with the undoped TiO_2, has been measured by UV-visible diffuse reflectance spectra, as shown in Figure **5a**. With regard to all the samples, an intense UV absorption

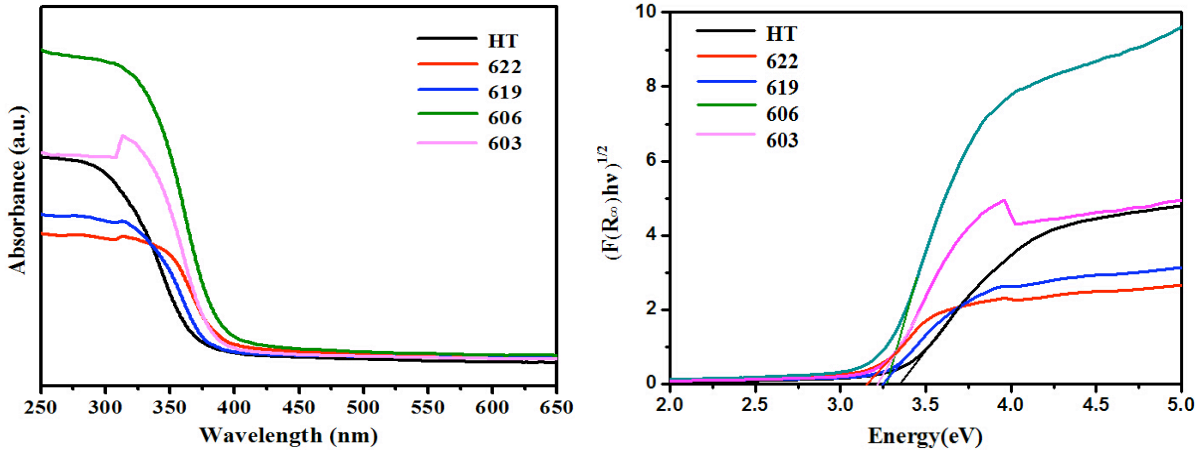

(**a**) (**b**)

Figure 5: The UV-Vis diffuse reflectance spectra (DRS) of C-N-S tridoped TiO_2 catalysts with different flyer velocities (**a**), and the plot of transformed Kubelka-Munk function versus the energy of light (**b**).

band appears from 250 nm to ca. 400 nm, which can be primarily ascribed to electrons promotion of TiO_2 from the valence band to the conduction band. However, 622 and 619 samples with the flyer velocity of 3.07 $km \cdot s^{-1}$ display lower intensity of ultraviolet absorption than metatitanic acid (HT), suggesting that the enhancement of shock loading may adversely affect the electronic structure of synthesized samples. It is interesting to observe that the C-N-S tridoped TiO_2 nanoparticles possess much better visible light absorption intensity than undoped TiO_2 (HT), indicating that they may have higher photocatalytic activity for a target reaction under visible light irradiation, especially the 606 and 603 ones. The red shift is ascribed to the fact that C-N-S tridoping can narrow the band-gap of the titania by mixing the orbit O 2p with C 2p, N 2p and S 3p orbits [13]. The improvement of absorbance in the UV-Vis region can increases the number of photogenerated electrons and holes to participate in the photocatalytic reaction, which can enhance the photocatalytic activity of TiO_2 [35]. Based on the optical absorption edge obtains from the UV-Vis DRS, the band gap energies (E_g) of different samples are calculated according to the plot in Figure **3b**, which is obtained *via* the transformation based on the Kubelka-Munk function [36]. The estimated band gap values of 622, 619, 606 and 603 samples are approximately 3.16, 3.24, 3.27 and 3.20 eV, respectively, clearly showing a band gap narrowing as compared to the estimated 3.36 eV of the undoped TiO_2 (HT). Therefore, it can be concluded that the doping elements of C, N, and S have a crucial effect on the optical properties of the TiO_2 photocatalysts.

3.4. Photocatalytic Activity

The photocatalytic activity of different samples is evaluated by photocatalytic degradation of Rhodamine B aqueous solution, as illustrated in Figure **6**. For comparison, the photocatalytic activity of raw material metatitanic acid (HT) and shock induced undoped TiO_2 (497) is also measured. The photocatalytic degradation efficiencies of the as-synthesized TiO_2 are summarized in Table **2**. Under dark conditions without light illumination, the concentration of RB almost does not change in the presence of majority samples. Therefore, the presence of both illumination and photocatalyst is necessary for the photocatalytic reaction to proceed. Obviously, Figure **6a** shows that the C-N-S tridoped TiO_2 samples exhibit higher photocatalytic activity compared with the behavior of raw metatitanic acid (HT) and shock induced undoped TiO_2 (497) under simulated sunlight irradiation. The degradation activities of the as-synthesized TiO_2 in the visible-light region are gradually improved in the order of 603 > 606 > 619 > 622, which are tuned by the dopant content and shock loading. Combined with the data in Table **2**, it can be seen that with increasing the mass ratios of TU/HT of dopant, the specific surface area of the samples increases and the photocatalytic activity of C-N-S tridoped TiO_2 photocatalysts is enhanced accordingly, while the photocatalytic degradation efficiencies of sample 619 and 622 decline when the flyer velocity rises to 3.07 $km \cdot s^{-1}$, that might be explained as threshold value exists in the process of modification induced by shock wave. Higher impact energy may generate a lot of residual strain and dislocation defect and decrease the crystallinity leading to the deterioration of catalytic activity, the 603 sample

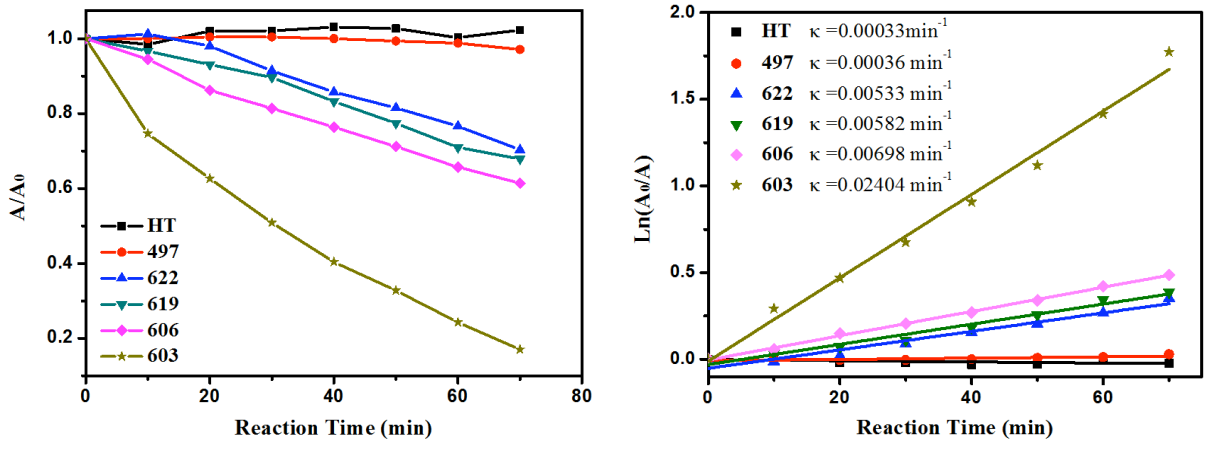

(**a**) (**b**)

Figure 6: Photocatalytic degradation curves (**a**) and fitted reaction rate curves (**b**) of C-N-S tridoped TiO_2 photocatalysts and the undoped TiO_2 under visible light irradiation.

after being treated at the optimal pressure and temperature possesses the better crystallinity and has higher specific surface area and narrower band gap and thus exhibits the best visible light photocatalytic activity with 83% of RB removal after 70 min of visible-light irradiation. The degradation of dyes can be ascribed to a pseudo-first-order reaction with a simplified Langmuir-Hinshelwood model: $\ln (A_0/A)=\kappa t$ [37], where κ is the apparent first-order rate constant. As displayed in Figure **6b**, the C-N-S tridoped TiO_2 (603) exhibits the highest photocatalytic activity with the kinetic rate constant (0.024 min^{-1}) under simulated sunlight irradiation. The enhancement of photocatalytic activity of C-N-S tridoped TiO_2 induced by shock wave is mainly attributed to the synergistic effects of well-formed anatase phase, high specific surface area and band gap narrowing resulting from C-N-S tridoping.

4. CONCLUSIONS

In summary, C-N-S tridoped TiO_2 nano-particles are assembled by shock induced chemical reaction of carbon, nitrogen, and sulfur dopant thiourea in situ. Metatitanic acid transforms to well-formed anatase phase TiO_2 with small particle size (3-5nm) and large specific surface area (309.02 m^2/g) under shock wave action. The photocatalytic activity of the samples improve significantly with thiourea content increasing and achieve the highest 83% removal rate under the visible light irradiation for 70min with the thiourea-to-metatitanic acid mass ratio of 2:1 and flyer velocity 2.52 $km{\cdot}s^{-1}$. Best treatment condition is existed in the process of doping modification induced by shock wave and the enhancement of photocatalytic activity is mainly attributed to the synergistic effects of well-formed anatase phase, high specific surface area and band gap narrowing resulting from C-N-S tridoping. The present experimental results suggest that the shock doping is a new and effective method to get TiO_2 photocatalyst responding to visible light.

ACKNOWLEDGEMENTS

The authors of this paper acknowledge the financial support from the National Natural Science Foundation of China (Grants 10972039 and 11172043), the Doctoral Funds of the Ministry of Education of China (Grant 200800070033), and the joint funds of the Beijing Municipal Commission of Education.

REFERENCES

[1] Fujishima A, Honda K. Electrochemical photolysis of water at a semiconductor electrode. Nature 1972; 238: 37-8. http://dx.doi.org/10.1038/238037a0

[2] Regan BO, Gratzel M. A low-cost, high-efficiency solar-cell based on dye-sensitized colloidal TiO_2 films. Nature 1991; m353: 737-40. http://dx.doi.org/10.1038/353737a0

[3] Bae EY, Choi WY. Highly enhanced photoreductive degradation of perchlorinated compounds on dye-sensitized metal/TiO_2 under visible light. Environ Sci Technol 2003; 37: 147-52. http://dx.doi.org/10.1021/es025617q

[4] Bamwenda GR, Tsubota S, Nakamura T, Haruta M. Photoassisted hydrogen production from a water-ethanol solution: a comparison of activities of Au-TiO_2 and Pt-TiO_2. J Photochem Photobiol. A Chem 1995; 89: 177-89. http://dx.doi.org/10.1016/1010-6030(95)04039-I

[5] Kohtani S, Kudo A, Sakata T. Spectral sensitization of a TiO_2 semiconductor electrode by CdS microcrystals and its photoelectrochemical properties. Chem Phys Lett 1993; 206: 166-70. http://dx.doi.org/10.1016/0009-2614(93)85535-V

[6] Asahi R, Morikawa T, Ohwaki T, Aokl K, Taga Y. Visible-Light Photocatalysis in Nitrogen-Doped Titanium Oxides. Science 2001; 293: 269-71. http://dx.doi.org/10.1126/science.1061051

[7] Yuan JJ, Li HD, Gao SY. Hydrothermal synthesis, characterization and properties of TiO_2 nanorods on boron-doped diamond film. Mater Lett 2010; 64: 2012-5. http://dx.doi.org/10.1016/j.matlet.2010.06.033

[8] Neumann B, Bogdanoff P, Tributsch H, Sakthivel S, Kisch H. Electrochemical mass spectroscopic and surface photovoltage studies of catalytic water photooxidation by undoped and carbon-doped titania. J Phys Chem B 2005; 109; 16579-86. http://dx.doi.org/10.1021/jp051339g

[9] Hirakawa T, Nosaka Y. Selective production of superoxide ions and hydrogen peroxide over nitrogen-and sulfur-doped TiO_2 photocatalysts with visible light in aqueous suspension systems. J Phys Chem C 2008; 112: 15818-23. http://dx.doi.org/10.1021/jp8055015

[10] Pan JH, Zhang XW, Du AJH, Sun DD, Leckie JO. Self-etching reconstruction of hierarchically mesoporous F-TiO_2 hollow microspherical photocatalyst for concurrent membrane water purifications. J Am Chem Soc 2008; 130: 11256-7. http://dx.doi.org/10.1021/ja803582m

[11] Tian H, Ma JF, Li K, Li JJ. Hydrothermal synthesis of S-doped TiO_2 nanoparticles and their photocatalytic ability for degradation of methyl orange. Ceram Int 2009; 35: 1289-92. http://dx.doi.org/10.1016/j.ceramint.2008.05.003

[12] Rengifo-Herrera JA, Pierzchala K, Sienkiewicz A, Forro L, Kiwi J, Pulgarin C. Abatement of organics and *escherichia coli* by N, S co-doped TiO_2 under UV and visible light. implications of the formation of singlet oxygen ($^1O_2$) under visible light. Appl Catal B: Environmental 2009; 88: 398-406. http://dx.doi.org/10.1016/j.apcatb.2008.10.025

[13] Zhou M, Yu J. Preparation and enhanced daylight-induced photocatalytic activity of C,N,S-tridoped titanium dioxide powders. J Hazard Mater 2008; 152: 1229-36. http://dx.doi.org/10.1016/j.jhazmat.2007.07.113

[14] Thadhani NN. Shock-induced chemical reactions and synthesis of materials. Prog Mater Sci 1993; 37: 117-226. http://dx.doi.org/10.1016/0079-6425(93)90002-3

[15] Ohno T, Akiyoshi M, Umebayashi T, Asai K, Mitsui T, Matsumura M. Preparation of S-doped TiO_2 photocatalysts and their photocatalytic activities under visible light. Appl Catal A: Gneral 2004; 265: 115-21. http://dx.doi.org/10.1016/j.apcata.2004.01.007

[16] Sato S, Nakamura R, Abe S. Visible-light sensitization of TiO_2 photocatalysts by wet-method N doping. Appl Catal A 2005; 284: 131-7. http://dx.doi.org/10.1016/j.apcata.2005.01.028

[17] Pore V, Heikkila M, Ritala M, Leskela M, Areva S. Atomic layer deposition of $TiO_{2-x}N_x$ thin films for photocatalytic applications. J Photochem Photobiol A: Chem 2006; 177: 68-75. http://dx.doi.org/10.1016/j.jphotochem.2005.05.013

[18] Chen PW, Gao X, Liu JJ, Zhou Q, Huang F. Shock-induced high-concentration nitrogen doping of titania. Combust Explo Shock 2012; 48: 724-9. http://dx.doi.org/10.1134/S0010508212060111

[19] Gao X, Chen PW, Liu JJ. Enhanced visible-light absorption of nitrogen-doped titania induced by shock wave. Mater Lett 2011; 65: 685-7. http://dx.doi.org/10.1016/j.matlet.2010.11.020

[20] Gao X, Liu JJ, Chen PW. Nitrogen-doped titania photocatalysts induced by shock wave, Mater. Res Bull 2009; 44: 1842-5. http://dx.doi.org/10.1016/j.materresbull.2009.05.020

[21] Liu JJ, Sekine T, Kobayashi T. A new carbon nitride synthesized by shock compression of organic precursors. Solid State Commun 2006; 137: 21-5. http://dx.doi.org/10.1016/j.ssc.2005.10.022

[22] Kamisaka H, Adachi T, Yamashita K. Theoretical study of the structure and optical properties of carbon- doped rutile and anatase titanium doxides. J Phys Chem 2005; 123: 084704. http://dx.doi.org/10.1063/1.2007630

[23] Wang PH, Yap PS, Lim TT. C-N-S tridoped TiO_2 for photocatalytic degradation of tetracycline under visible-light irradiation. Appl Catal A 2011; 399: 252-61. http://dx.doi.org/10.1016/j.apcata.2011.04.008

[24] Cheng XW, Yu XJ, Xing ZP. One-step synthesis of visible active C-N-S-tridoped TiO_2 photocatalyst from biomolecule cysteine. Appl Surf Sci 2012; 258: 7644-50. http://dx.doi.org/10.1016/j.apsusc.2012.04.111

[25] Suda Y, Kawasaki H, Ueda T, Ohshima T. Preparation of high quality nitrogen doped TiO_2 thin film as a photocatalyst using a pulsed laser deposition method. Thin Solid Films 2004; 453-454: 162-6. http://dx.doi.org/10.1016/j.tsf.2003.11.185

[26] Randeniya LK, Murphy AB, Plumb IC. A study of S-doped TiO_2 for photoelectrochemical hydrogen generation from water. J Mater Sci 2008; 43: 1389-99. http://dx.doi.org/10.1007/s10853-007-2309-z

[27] Wang YW, Huang Y, Ho WK, Zhang LZ, Zou ZG, Lee SC. Biomolecule-controlled hydrothermal synthesis of C-N-S-tridoped TiO_2 nanocrystalline photocatalysts for NO removal under simulated solar light irradiation. J Hazard Mater 2009; 169: 77-87. http://dx.doi.org/10.1016/j.jhazmat.2009.03.071

[28] Wei F, Ni L, Cui P. Preparation and characterization of N-S-codoped TiO_2 photocatalyst and its photocatalytic activity. J Hazard Mater 2008; 156: 135-40. http://dx.doi.org/10.1016/j.jhazmat.2007.12.018

[29] Yang GD, Yan ZF, Xiao TC. Low-temperature solvothermal synthesis of visible-light-responsive S-doped TiO_2 nanocrystal. Appl Surf Sci 2012; 258: 4016-22. http://dx.doi.org/10.1016/j.apsusc.2011.12.092

[30] Feng ND, Zheng A, Wang Q, Ren PP, Gao XZ, Liu SB, *et al*. Boron environments in B-doped and (B, N)-codoped TiO_2 photocatalysts: a combined solid-state NMR and theoretical calculation study. J Phys Chem C 2011; 115: 2709-19. http://dx.doi.org/10.1021/jp108008a

[31] Bacsa R, Kiwi John, Ohno T, Albers P, Nadtochenko V. Preparation, testing and characterization of doped TiO_2 active in the peroxidation of biomolecules under visible light. J Phys Chem B 2005; 109: 5994-6003. http://dx.doi.org/10.1021/jp044979c

[32] Vijayan BK, Dimitrijevic NM, Wu J, Gray KA. The effects of Pt doping on the structure and visible light photoactivity of titania nanotubes. J Phys Chem C 2010; 114: 21262-9. http://dx.doi.org/10.1021/jp108659a

[33] Ju J, Chen X, Shi Y, Miao J, Wu D. Hydrothermal preparation and photocatalytic performance of N, S-doped nanometer TiO_2 under sunshine irradiation. Powder Technol 2013; 237: 616-22. http://dx.doi.org/10.1016/j.powtec.2012.12.048

[34] Ohno T, Akiyoshi M, Umebayashi T, Asai K, Mitsui T, Matsumura M. Preparation of S-doped TiO_2 photocatalysts and their photocatalytic activities under visible light. Appl Catal A: General 2004; 265: 115-21. http://dx.doi.org/10.1016/j.apcata.2004.01.007

[35] Li D, Haneda H, Hishita S, Ohashi N. Visible-light-driven nitrogen-doped TiO_2 photocatalysts: effect of nitrogen precursors on their photocatalysis for decomposition of gas-phase organic pollutants. Mater Sci Eng B 2005; 117: 67-75. http://dx.doi.org/10.1016/j.mseb.2004.10.018

[36] Serpone N, Lawless D, Khairutdinov R. Size effects on the photophysical properties of colloidal anatase TiO_2 particles: size quantization or direct transitions in this indirect semiconductor. J Phys Chem 1995; 99: 16646-54. http://dx.doi.org/10.1021/j100045a026

[37] Xu YJ, Zhuang YB, Fu XZ. New insight for enhanced photocatalytic activity of TiO_2 by doping carbon nanotubes: A case study on degradation of benzene and methyl orasnge. J Phys Chem C 2010; 114: 2669-76. http://dx.doi.org/10.1021/jp909855p

Received on 17-02-2015 Accepted on 01-03-2015 Published on 14-07-2015

DOI: http://dx.doi.org/10.15377:2410-4701.2015.02.01.3